SIMULATION OF THE ELECTRIC FIELD IN A SUBMERGED ARC FURNACE

M. Dhainaut

SINTEF Materials Technology, Alfred Getz vei 2B, N-7465 Trondheim, Norway.
E-mail: Marc.Dhainaut@sintef.no

ABSTRACT

This paper presents computations of the electric field inside a furnace. We first look at the effect of contact between two coke particles from an electrical point of view. We give values for the amount of contact resistance in the total resistance of the system formed by the two coke particles. We show that the effect of contact resistance decreases rapidly with increasing contact area. We then look at the complete electric field inside a full scale furnace. The aim is to evaluate the amount of current that short-cuts the metal bath for different vertical positions of the electrodes. We show that electrodes high above the metal bath are undesirable since they offer a larger surface of conductive charge materials where current can flow through. On the other hand, deeper electrodes force the current to go the whole way down to the metal bath. Ohmic heating along this path ensures a high temperature of coke and slag that are beneficial for metal recovery.

1. INTRODUCTION

The knowledge we have today on electrical furnaces is primarily based on experience from operating plants and from experimental work on small scale furnaces. These approaches are necessary and often valuable when one needs to investigate special issues related to the furnace. However, they are expensive, time demanding and never really satisfactory since it is not possible to control all the parameters that make the furnace works as it does.

Numerical simulation on the other hand works on models. This allows one to fully control the different parameters involved in the model and to easily investigate various issues that will help to understand or predict the state of operation of a furnace.

At the research foundation SINTEF, we are developing a tool that will simulate the main mechanisms that take place inside a ferromanganese and silicomanganese furnace. This tool is built on Fluent© [1], a major Computational Fluid Dynamics software product. The use of CFD is explained by the fact that non trivial transport of mass, momentum and energy occurs in a furnace where different phases (gas, liquid, solid) are flowing and reacting. Our goal is to integrate the slag and gas flow field, the electrical field, the temperature field and the kinetics of the chemical reactions in the simulations.

This paper presents some results obtained from the use of the electric field model. It is divided into three parts. The first part gives the equations governing the electrical and thermal field. The second part focuses on the effect of contact between two coke particles from an electrical point of view. The third part shows an example on how this model can be used to simulate and predict the electrical field inside a furnace.

2. THEORY

The electric field model solves the Ohm's law and the continuity equation (conservation of charge):

$$\vec{j} = -\sigma \nabla \phi \tag{1}$$

$$\frac{\partial q}{\partial t} + div\left(\vec{j}\right) = 0 \tag{2}$$

Proceedings: Tenth International Ferroalloys Congress;
INFACON X: '*Transformation through Technology*'
ISBN: 0-9584663-5-1

1 – 4 February 2004
Cape Town, South Africa
Produced by: Document Transformation Technologies

where j [A/m^2] is the current density, σ [S/m] is the electrical conductivity of the medium and ϕ [V] is the electric potential. q [C/m^3] is the charge density. The term $\partial q/\partial t$ in Equation 2 is negligible since the variation of q with time is based on time scales (10^{-14}-10^{-15} s) that are much smaller than the one of the electrical furnace, which operates with alternating current of frequency f = 50 Hz, i.e. of period 20 ms. The criterion $2\pi.f.\varepsilon/\sigma_{coke} << 1$ that states that displacement (or capacitive) current density is much smaller than conduction current density is fulfilled by f and the harmonics of importance (ε and σ_{coke} are respectively the permittivity and the electrical conductivity of coke) [2]. A quasi-stationary approach can thus be applied and Equation 2 is written in its stationary form:

$$div\left(\vec{j}\right) = 0 \tag{3}$$

The thermal field is governed by the energy equation written as:

$$\frac{\partial}{\partial t}(\rho h) = div(k\nabla T) + \frac{j^2}{\sigma} \tag{4}$$

where h [J/kg] is the specific enthalpy and T [K] the temperature. ρ [kg/m^3] is the density and k [W/m-K] the thermal conductivity of the material.

The electric and thermal fields are coupled via the Joule term j^2/σ .
Although our electric field model is implemented using equation 1, 3 and 4, we will only present steady computations in this paper and therefore, Equation 4 will be used in its stationary form:

$$0 = div(k\nabla T) + \frac{j^2}{\sigma} \tag{5}$$

These equations are implemented in Fluent© (version 6) and solved using a Finite Volume approach. The potential, the current density and the temperature are co-located (i.e. they are all computed at the centre of the grid cells). Structured, unstructured, hexahedral and tetrahedral grid mesh can be used.

The model has been tested for geometries where analytical solutions could be found and compared very accurately.

3. STUDY OF PARTICLE CONTACT

The study of contact between coke particles is important because the electric current will preferentially flow along paths made exclusively of coke since coke usually has a higher conductivity than slag. At the contact point between two coke particles, the current density reaches very high values because of the concentration of current through this small contact area. The smaller the contact area, the higher the resistance at this point. By Joule effect, the temperature at the contact point increases significantly and since coke thermal and electrical conductivity increase with temperature the contact point is heated up until it eventually disappears after being consumed. The electrical current needs then to find a new path.

3.1 The physical model

We study here the effect of the contact area on the total resistance of an object which geometry represents two pieces of coke getting progressively closer. Figure 1 shows the geometry representing the two pieces as we increase their area of contact (a, b, c, and d). The computations are made in 2D which means that the depth of the pieces is 1. Each piece is made of a half disk (diameter of dimensionless size 1) mounted on a square (1 x 1). When the disks of the two pieces have an ideal point as contact, the length of the total object is 3 (Figure 1.a). The geometries of Figure 1.b and 1.c are obtained by translating vertically the two pieces closer to each other. This would represent two coke particles having a non-zero contact area. During this translation, the two half disks partially merge and the length of the total object decreases as the contact width increases, until the contact width exactly equals the width of the square (Figure 1.d) since the two half disks have completely merged.

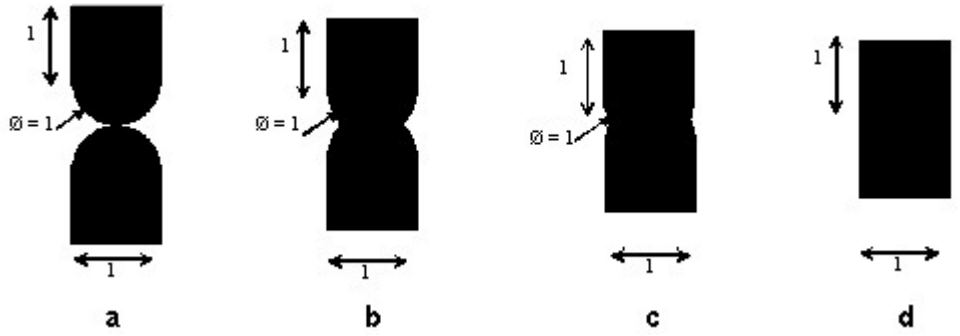

Figure 1. Two coke particles are progressively merged increasing their contact width (or area in 3D).

For each geometry representing a particular position of the two pieces, we compute the total resistance of the sample (calling "sample" the two pieces in contact) for which we apply a voltage of 1V at the top and 0V at the bottom. The side walls are insulated. Concerning the temperature field, we assume a constant temperature at the top and the bottom of the sample (T = 300°K) while the side walls are adiabatic.

3.2 The contact resistance

The resistance of the sample will obviously decrease as the two pieces get closer to each other. This is due to the fact that the contact width increases offering less resistance but also because the total length of the object decreases. How to focus only on the effect of contact width? The problem here is to define a "contact resistance". There is no obvious and immediate definition of what a "contact resistance" is. We define hereafter the contact resistance as the difference between the total resistance of the sample and the resistance of a rectangle (or brick in 3D) of same length and surface area (or volume in 3D) as the sample. The width of the rectangle is constrained by these requirements. Figure 2 shows the equivalent rectangles corresponding to the samples drawn in Figure 1.

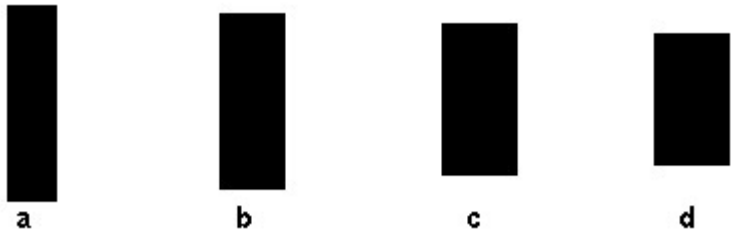

Figure 2. Reference objects for the computation of contact resistance of the samples of Figure 1. These rectangles have same length and surface area (or volume in 3D) as their corresponding samples of Figure 1.

The rectangles have the same electrical and thermal boundary conditions as the samples (i.e. a potential gradient of 1V is applied between the top and bottom of the rectangles while the side walls see no electrical or thermal fluxes).

The computations are performed for a material having one of the following electrical conductivities, σ :

- constant conductivity

$$\sigma = 5000 \quad [\text{S/m}] \tag{6}$$

- increasing conductivity with temperature

$$\sigma = \frac{5000}{300} T \quad [\text{S/m}] \tag{7}$$

decreasing conductivity with temperature

$$\sigma = \frac{5000 \times 300}{T} \quad [\text{S/m}] \tag{8}$$

The temperature dependency of the conductivity is such that at T = 300°K, the conductivity of all the samples is equal to 5000 S/m.

Figure 3 shows the evolution of the contact resistance as a function of the contact width (or area in 3D) for the different conductivities written above. The contact width is given in percent of the total width of the sample. That is: 0% corresponds to an ideal contact point of zero dimension (Figure 1.a), while 100% corresponds to a contact width equal to the sample width, i.e. 1, (Figure 1.d).

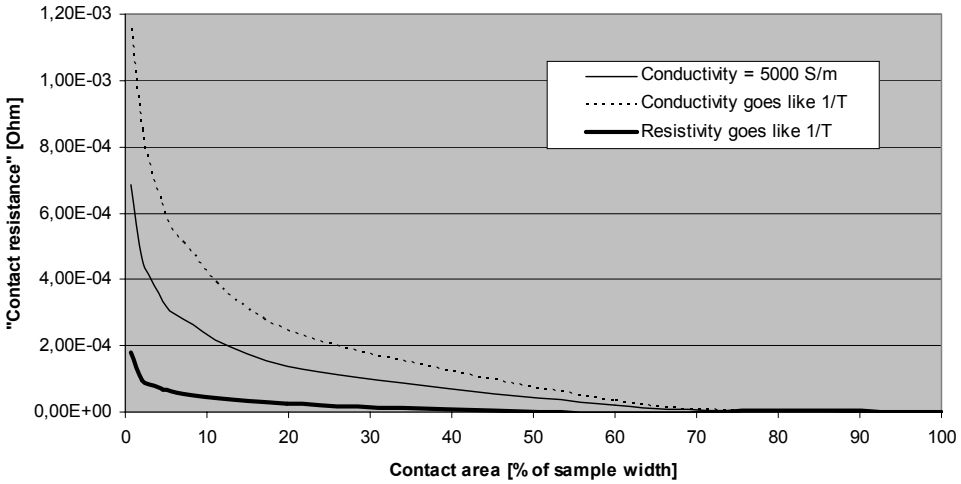

Figure 3. Contact resistance as a function of contact area for different electrical conductivity temperature dependency.

We can see that, for a given contact width, the contact resistance reaches lower values when the conductivity is an increasing function of temperature. This is natural since, for this temperature dependency, ohmic heating at the contact between the two particles will significantly increase the conductivity there. However, the three curves are difficult to compare any further because they do not present the same temperature levels. An interesting observation can be made from Figure 4 where instead of looking at the contact resistance as an absolute value, we look at the percentage of the contact resistance in the total resistance of the sample. This tells us how much does the contact resistance contribute to the total sample resistance.

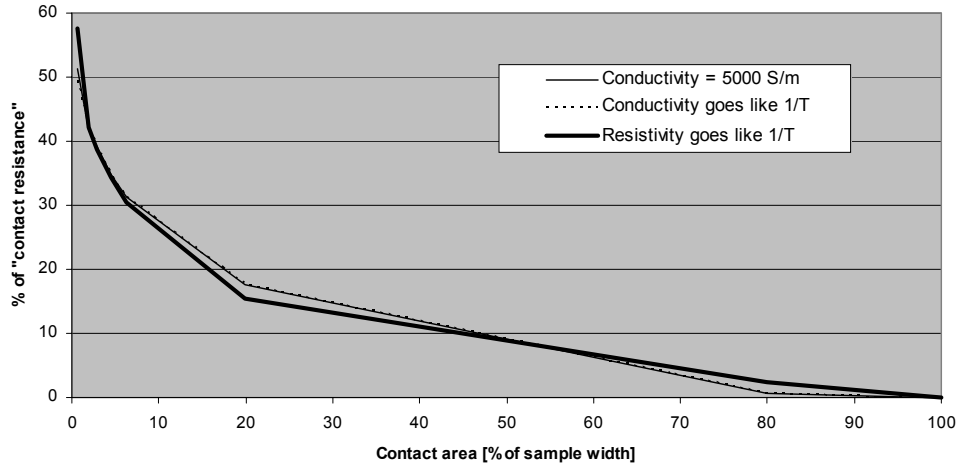

Figure 4. Amount of contact resistance in the total resistance of the sample as a function of contact width.

The three curves are almost coincident. This means that the “contact resistance” represents the same amount of the total resistance whatever the electrical conductivity dependency with temperature. Therefore, the relative effect of contact resistance is a pure geometrical issue that does not depend on material data. For very small contact zones (some percent of the typical size of the sample), the contact resistance makes of course most of the total resistance of the sample. However, the effect of contact resistance decreases rapidly with the increase in contact area. For a contact width being for example one fifth of the sample width, the contact resistance accounts only for 15% of the total resistance of the sample.

3.3 Non-sinusoidal currents

When a sinusoidal voltage is applied to the sample, the current is also sinusoidal if the resistance of the material is independent of the voltage. However, as coke electrical conductivity is temperature dependent (and therefore voltage dependent), the current shows a periodic signal of same fundamental frequency as the voltage, but perturbed by over-harmonics. This is a well known phenomenon observed in situ. The over-harmonics can also be observed in the computations.

The computations use as input a succession of steady state voltages, without dynamic effects (time relaxation). Voltage is given as a series of values that follow a sinusoid. For each of these values, the steady-state potential field and corresponding current are computed.

The two pieces have a contact area of 0.64%, i.e. almost point contact, although the same kind of results are obtained for any contact area since the over-harmonics appear whenever the electrical conductivity is temperature dependent. The effect of the contact area is in the amplitude reached by the over-harmonics. The current response from a sinusoidal voltage is given in Figure 5.

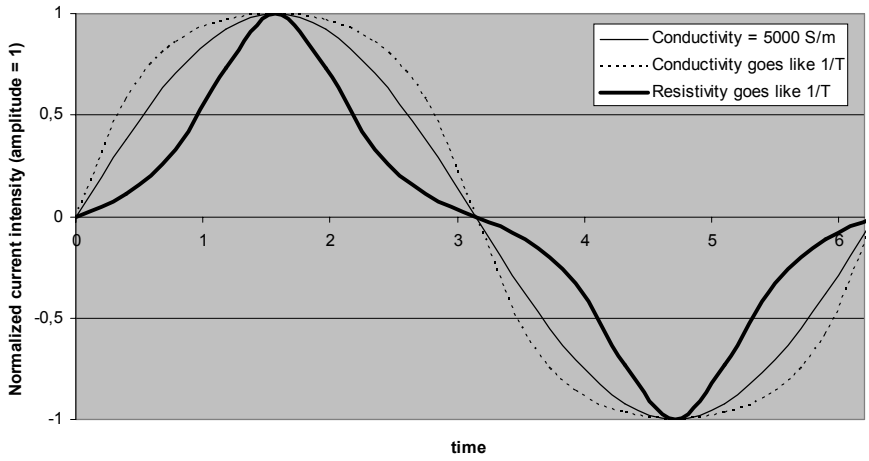

Figure 5. Visualization of the over-harmonics found in a sample with temperature dependent conductivity.

For a constant conductivity, the current response is of course a sinusoid (thin line). When conductivity is temperature dependent the over-harmonics appear (dashed line and thick line).

4. 3D SIMULATION OF THE ELECTRIC FIELD IN A FURNACE

The electric field model can be used to study problems at the scale of particles like in the previous section, but also at the scale of a real furnace. In this section, we look at the electric field inside a furnace for different vertical positions of the electrodes.

4.1 The geometry

An industrial furnace has been used to build our geometrical model. The dimensions of this furnace are:

- Electrode diameter: 1.9 m
- Distance between electrodes: 4.4 m
- Furnace diameter: 10.3 m
- Furnace height: 5 m
- Electrode height: variable (the electrode tips are 1 m or 3 m above the metal bath)

The aim is to map the different paths the electrical current follows to go from one electrode to another. The computation does not consider the temperature field yet, but will, when the model will incorporate the complete energy balance where enthalpy from chemical reactions will be accounted for.

Several simple analytical models for the calculation of furnace resistance from specific resistivity of the mix components have been attempted (see for example Downing and Urban [3]). Healy ([4], [5]) considered that the current flowing from the electrodes to the hearth follows concentric hemispherical shells. He considered constant mix resistivity. These assumptions led him to an analytical expression of the total current. In reality, the bending of the streamlines of current will depend among others on the height of the electrodes and on how the different layers of material (mixture, slag, coke-bed) are arranged inside the furnace.

The computations we present here make no assumption for the current path. It is a result of the computations. Concerning the arrangement of the different layers of materials inside the furnace, we assume that the furnace is made of three electrodes, three mixture zones of ores and coke having each a constant characteristic temperature (increasing when approaching the hearth of the furnace), one hearth (mixture of coke and molten slag) and the metal bath. The schematic of this furnace partitioning is presented in Figure 6 below for electrode tips being 1 m (left figure) and 3 m (right figure) over the metal bath.

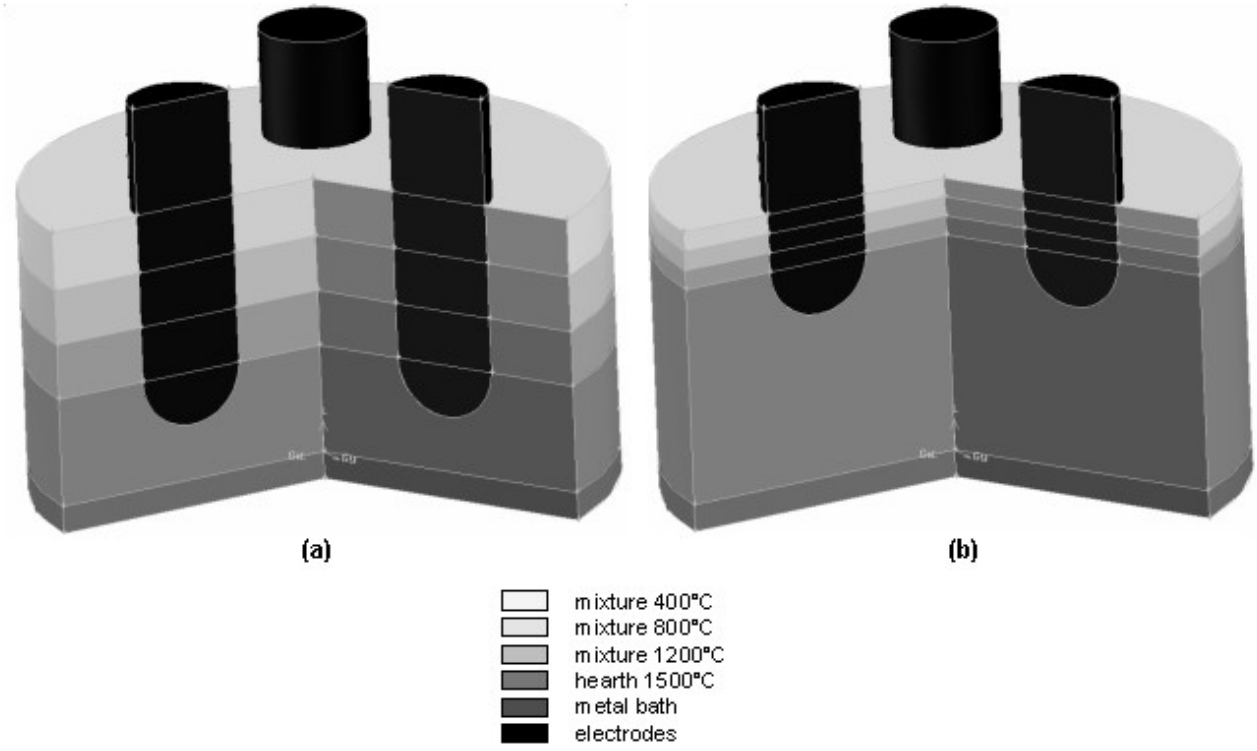

Figure 6. Schematic of the furnace partitioning for electrode tips positioned 1 m (Fig. 6.a) and 3 m (Fig. 6.b) over the metal bath. (For black and white prints of the pictures: from top to bottom, colours get darker).

The assumed temperature of each zone (i.e. T= 400°C, 800°C, 1200°C, and 1500°C) and their corresponding colour are indicated below the two pictures of the furnace. The 1500°C zone is considered to be the hearth of the furnace where molten slag reacts with coke to form molten metal. This zone is situated between the electrode tips and the metal bath. That is why for electrode tips being 1 m over the metal bath this zone is rather small compared to the situation where the electrode tips are positioned 3 m over the metal bath.

This partitioning of the furnace is not without resemblance to the one used by Urquhart *et al.* [6] for estimating the electric power dissipated in the burden of the furnace. However, the geometry of the mixture of ores and coke is of course more complex than the “slices” shown in Figure 6. With the help of Computer Aided Design, there is virtually no limit in how complex the geometry of the furnace can be modelled and simulated. Like [6], we assume only ohmic conduction inside the furnace. Possible arcing between particles is not taken into account.

Finally, it is to be mentioned that the full model of Figure 6 has been shown for clarity but only half of the model is really computed since the furnace carries a vertical symmetry plane that saves computational time.

4.2 Material data and boundary conditions

Each of the zones defined above are supposed to have a constant electrical resistivity. The resisitivity of the ore and coke mixtures at different temperature are taken from Miyauchi *et al.* [7]. He measured the electrical conductivity of mixtures of manganese ores and coke for the production of high carbon ferromanganese. These values were relative to coke resistivity. We assume that coke resistivity at 1500°C is 6.7 mΩ.m and that this resistivity corresponds to the hearth at 1500°C, which is made of coke and molten slag. This value is in the order of the one found for the real ferromanganese furnace we are simulating. According to the data from [7], the mixtures at 1200°C, 800°C and 400°C are about 10 times, 1000 times, and 2000 times more resistive than that. The electrodes and the metal bath are much more conductive than any of these materials. For the computation, we assume they are 1000 times more conductive than the hearth at 1500°C. Table 1 below summarises the material data used for the computations.

Table 1. Electrical resistivity and conductivity of the different zones in the furnace.

Homogeneous zones of the furnace	electrical resistivity [Ω.m]	electrical conductivity [S/m]
Mixture at 400°C	13.3	0.075
Mixture at 800°C	6.7	0.15
Mixture at 1200°C	$6.7.10^{-2}$	15
Hearth at 1500°C	$6.7.10^{-3}$	150
Electrodes	$6.7.10^{-6}$	150.10^{3}
Metal bath	$6.7.10^{-6}$	150.10^{3}

The furnace runs on three phase alternating current. It would be fully possible, although time-consuming, to compute the furnace with time-dependent current. We have instead decided to simulate only one instant of time where one electrode has a voltage of 100 V while the two others have a voltage of –50 V. It is therefore a stationary computation performed at a specified instant of time. Any other instant of time could have been chosen, but this one makes it easier to visualise the current path since it carries some symmetry.
The walls of the furnace are insulated, and therefore no current goes through the walls.

4.3 Results from the computations of the current distribution in the furnace

The computation of the electric field inside the furnace gave a total current of 145 and 115 kA for electrode tips positioned respectively 1 m and 3 m above the metal bath. The total electrode resistance is 0.7 and 0.9 mΩ respectively. These values are within the order of magnitude observed at operating ferromanganese furnaces. The distribution of the current is shown in Figure 7 below for the two vertical positions of the electrodes.

When the furnace has its electrodes 1 m above the metal bath (Figure 7.a), the hearths at 1500°C belonging to the different electrodes have a small contact area and therefore most of the current goes through the metal bath (72%).

When the furnace has its electrodes 3 m over the metal bath, the hearths at 1500°C belonging to the different electrodes have a much larger contact area and most of the current (i.e. 63 %) short-cuts the metal bath and goes directly from one electrode to the other via coke and slag at 1500°C. This situation is undesirable since, among others, it reduces the ohmic heating of coke and slag in the bottom of the furnace. The metal surface gets colder complicating the tapping of the furnace.

The current flowing through the hearth and charge has also a self-enhancing effect: since more current goes through the charge, the charge is heated up (ohmic heating) increasing the conductivity of the materials and again increasing the amount of current flowing directly through it. This thermal effect will be studied as soon as we introduce a new energy term in Equation 5 that accounts for the enthalpy of the chemical reactions inside the furnace. This is the next step for the development of our model.

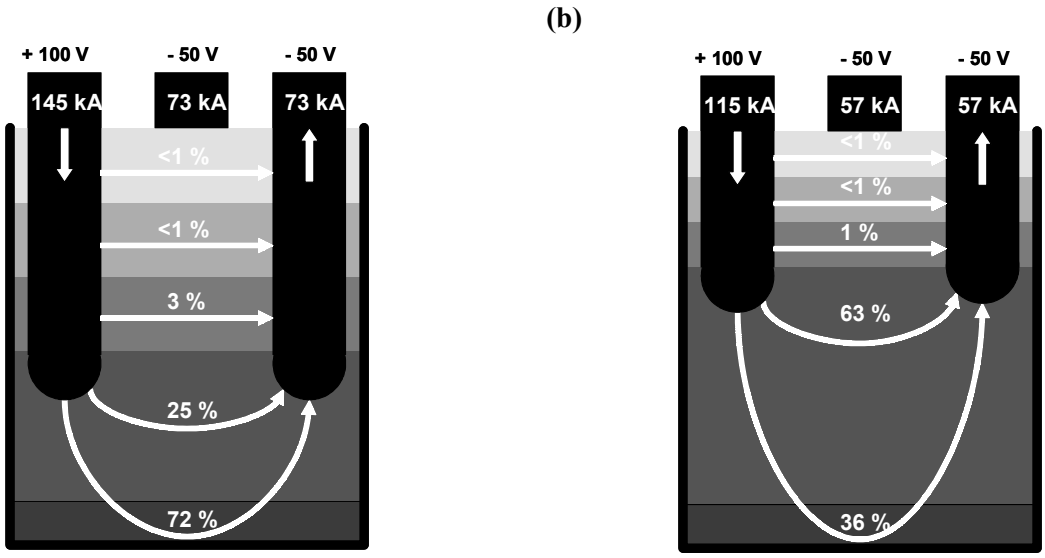

Figure 7. Illustration of the different paths used by the current to go from one electrode to the others for two situations: electrode tips are 1 m over the metal bath (Fig.7.a) and electrode tips are 3 m over the metal bath (Fig.7.b).

5. CONCLUSION

This paper presented some results from the computations of the electric field in a furnace.

On the meso-scale, we studied the effect of particle contact on the electrical resistance. We gave a definition of contact resistance and showed that only for rather small contact area does the contact resistance represent a large part of the total resistance. We also showed that this amount of contact resistance in the total resistance is not dependent on how sensitive the material conductivity is with temperature. The relative effect of contact resistance only depends on the size of the contact, and decreases rapidly for increasing contact area.

On the macro-scale, we presented results from the computation of the electric field inside a real ferromanganese furnace. The idea was to see how the electric field is affected by the vertical position of the electrodes. We confirmed the experimental results that higher electrodes are undesirable since they offer large paths where current can directly flow in, short-cutting the metal bath. The accuracy of the results obtained, partly depends on how well we describe the inside of the furnace. In this paper we have presented a quite simple geometrical model of the inside of the furnace, assuming that materials of different resistivity are arranged in horizontal layers.

The further development of the model will include the reaction kinetics to get the thermal field inside the furnace. Finally, we will compute the flow field, the electric field and the thermal field as a coupled system.

6. REFERENCES

[1] Fluent©: Fluent is a registered trademark of Fluent Incorporated, www.fluent.com .
[2] Lim Y.K., “Introduction to classical electrodynamics” World Scientific Publishing 1986.
[3] Downing J.H., Urban L., “Electrical conduction in submerged arc furnaces” Electric Furnace Conference Proceedings AIME, 1965, Vol.23, pp. 92-101.
[4] Healy G.W., “Ferromanganese material and energy balances, calculation of electrical resistance of mix” Proceedings of the international symposium on ferrous and nonferrous alloy processes, R.A. Bergman editor, pp.85-96, Pergamon Press, 1990.
[5] Healy G.W., “How ferromanganese mix resistivity affects manganese gas, carbon balance, and kWh per metric ton” Electric Furnace Conference Proceedings AIME, 1991, pp. 251-258.
[6] Urquhart R.C., Jochens P.R., Howat D.D., “The dissipation of electrical power in the burden of a submerged arc furnace” Electric Furnace Conference Proceedings AIME, 1973, Vol.31, pp. 73-78.
[7] Miyauchi Y., Mochida M., Fuchi Y., “High thermal property of manganese ore in production of high carbon ferromanganese.” Proceedings from the Ninth International Ferroalloys Congress, 2001, pp. 236-243.